Dust on Snow Radiative Forcing and Contribution to Melt in the Colorado River Basin

Patrick Naple; S. McKenzie Skiles; Otto I. Lang; Karl Rittger; Sebastien J. P. Lenard; Annie Burgess; Thomas H. Painter

AGU ADVANCING EARTH AND SPACE SCIENCES

Geophysical Research Letters

RESEARCH LETTER
10.1029/2024GL112757

Special Collection:
Analyzing Big Data for Understanding Climate Variability, Natural Phenomena and Rapid Environmental Changes

Key Points:

- Spatiotemporal patterns in dust on snow radiative forcing and melt contribution assessed over the MODIS period of record
- Dust darkens snow every year and impacts were generally higher in the first half of the record
- The dust on snow radiative impacts accelerate snowmelt every spring with relevant melt contribution even in lower magnitude years

Supporting Information:

Supporting Information may be found in the online version of this article.

Correspondence to:

S. M. Skiles,
m.skiles@utah.edu

Citation:

Naple, P., Skiles, S. M., Lang, O. I., Rittger, K., Lenard, S. J. P., Burgess, A., & Painter, T. H. (2025). Dust on snow radiative forcing and contribution to melt in the Colorado River Basin. *Geophysical Research Letters*, *52*, e2024GL112757. https://doi.org/10.1029/2024GL112757

Received 25 SEP 2024
Accepted 5 FEB 2025

Author Contributions:

Conceptualization: S. McKenzie Skiles, Thomas H. Painter
Data curation: Patrick Naple, S. McKenzie Skiles, Karl Rittger, Sebastien J. P. Lenard
Formal analysis: Patrick Naple
Funding acquisition: S. McKenzie Skiles, Karl Rittger, Thomas H. Painter
Investigation: S. McKenzie Skiles

Dust on Snow Radiative Forcing and Contribution to Melt in the Colorado River Basin

Patrick Naple[1], S. McKenzie Skiles[1], Otto I. Lang[1], Karl Rittger[2], Sebastien J. P. Lenard[2], Annie Burgess[3], and Thomas H. Painter[4,5]

[1]Snow Hydrology Research to Operations Laboratory, School of Environment, Society & Sustainability, University of Utah, Salt Lake City, UT, USA, [2]Institute of Arctic and Alpine Research, University of Colorado, Boulder, CO, USA, [3]Earth Science Department, Montana State University, Bozeman, MT, USA, [4]Joint Institute for Regional Earth System Science and Engineering, University of California – Los Angeles, Los Angeles, CA, USA, [5]Airborne Snow Observatories, Inc., Mammoth Lakes, CA, USA

Abstract In the mountainous headwaters of the Colorado River episodic dust deposition from adjacent arid and disturbed landscapes darkens snow and accelerates snowmelt, impacting basin hydrology. Patterns and impacts across the heterogenous landscape cannot be inferred from current in situ observations. To fill this gap daily remotely sensed retrievals of radiative forcing and contribution to melt were analyzed over the MODIS period of record (2001–2023) to quantify spatiotemporal impacts of snow darkening. Each season radiative forcing magnitudes were lowest in early spring and intensified as snowmelt progressed, with interannual variability in timing and magnitude of peak impact. Over the full record, radiative forcing was elevated in the first decade relative to the last decade. Snowmelt was accelerated in all years and impacts were most intense in the central to southern headwaters. The spatiotemporal patterns motivate further study to understand controls on variability and related perturbations to snow water resources.

Plain Language Summary Seasonal melt from mountain snowpacks dominates water resource availability in the Upper Colorado River Basin (UCRB). The mountainous Colorado River headwaters are adjacent to arid regions that regularly emit dust that darkens the snow. Darker snow melts earlier and faster due to the snowpack absorbing more of the sun's energy. This study uses 23 years of daily remotely sensed images to observe patterns in dust on snow impacts during the melt season across the UCRB. Results showed that impacts were greatest in the central-southern Rocky Mountains at mid-alpine elevations. Over time, snow darkening and accelerated melt were generally higher in the first half of the record with a slight declining trend across the full record. However, dust contributed to accelerating melt every spring over the record. Results suggest the need for further study to understand what controls dust on snow variability and magnitude of impact from year to year.

1. Introduction

The Colorado River system, which supplies water to over 40 million people across seven Western US states and two Mexican states, originates as snowmelt from the mountainous headwaters of the Upper Colorado River Basin (UCRB) (James et al., 2014). Due to the abundance of upwind arid and disturbed dust-producing landscapes, such as the southern Colorado Plateau, mountain snow in the UCRB is susceptible to surface darkening from mineral dust deposition (Painter et al., 2007). Deposited dust lowers snow albedo, increases absorbed solar radiation, and accelerates melt (Hock et al., 2019; Skiles et al., 2018). There is so much dust deposited in this region that it strongly dominates (>90%) concentrations and radiative impacts relative to other light absorbing particles (LAPs) like black carbon (Skiles & Painter, 2017, 2018). The amount of dust is related to human activity with deposition rates increasing by orders of magnitude following land use change and surface disturbance associated with modern settlement of the Western US (WUS) (Brahney et al., 2013; Neff et al., 2008). The timing and magnitude of snow darkening and impacts on melt rates are critical to understand across the Colorado River Basin, where snowmelt accounts for 85% of streamflow generation, on average (Barnett & Pierce, 2009; Jacobs et al., 2011; Rasmussen et al., 2012).

Observational studies at Senator Beck Basin Study Area (SBBSA), in the southwestern portion of the UCRB, document that dust on snow deposition has occurred every year since observations began in 2003, with most events occurring in the spring (Painter, Skiles, et al., 2012; Skiles et al., 2012; Skiles & Painter, 2017). Correspondingly, dust radiative forcing (RF_{dust}), the additional absorption of solar radiation due to surface darkening by

Methodology: S. McKenzie Skiles, Annie Burgess
Project administration: S. McKenzie Skiles
Resources: S. McKenzie Skiles
Software: Annie Burgess
Supervision: S. McKenzie Skiles
Validation: Patrick Naple, S. McKenzie Skiles
Visualization: Patrick Naple, S. McKenzie Skiles, Otto I. Lang
Writing – original draft: Patrick Naple
Writing – review & editing: S. McKenzie Skiles, Otto I. Lang, Karl Rittger, Sebastien J. P. Lenard, Annie Burgess, Thomas H. Painter

dust, generally increases between mid-March and mid-April as both surface dust concentrations and solar irradiance increase (Skiles et al., 2012; Skiles & Painter, 2017). The RF_{dust} impact is very effective at forcing faster snowmelt, accelerating snow depletion by 3–7 weeks, and acts as a primary control on snowmelt timing (Painter et al., 2018; Skiles et al., 2012). This has broad implications for water resources; earlier and more rapid melt forced by dust produces error in snowmelt forecasting and lower water yields downstream (Bryant et al., 2013; Painter et al., 2010).

The long-term in situ record of dust deposition timing, dust concentrations, and RF_{dust} has been valuable for process-based understanding of dust on snow processes and impacts. However, dust impacts documented at study areas are unlikely to be representative across the broad expanse of mountainous headwaters, which span multiple WUS states. This is a critical gap in our understanding of the hydrologic impacts of dust on snow in the Colorado River system. To address this, we evaluate spatial and temporal variability in dust impacts across the Colorado River headwaters from remote sensing over the MODIS period of record (2001–2023) using daily retrievals of RF_{dust} and contribution to melt, with the latter being a new metric to directly quantify impacts to snowmelt. This is the most comprehensive spatial and temporal evaluation of RF_{dust} to date.

2. Data and Methods

2.1. Remote Sensing Snow Products

Retrievals were analyzed from the Moderate Resolution Imaging Spectrometer (MODIS) Snow Cover Fraction and Grain Size (MODSCAG; Painter et al., 2009) and Dust Radiative Forcing in Snow (MODDRFS; Painter, Bryant, & Skiles, 2012) retrieval workflows. The snow retrievals are produced from the MODIS Terra Level 2 reflectance product (MOD09GA), a daily product that includes seven land bands at 463 m spatial resolution. To fill gaps due to clouds and carry out off-nadir correction, the spatially and temporally complete (STC) workflow was applied to produce daily, gap-filled, data sets over the MODIS record (STC-MODSCAG/MODDRFS) (Dozier et al., 2008; Jensen et al., 2024; Rittger et al., 2024).

The MODSCAG algorithm uses spectral mixture analysis to retrieve per pixel fractional snow cover (f_{sca}), used here to create a snow mask that defines the analysis area (Painter et al., 2009). The MODDRFS algorithm quantifies per-pixel snow darkening, defined as the reduction in visible albedo due to dust, and RF_{dust} (Painter, Bryant, & Skiles, 2012). First, effective snow grain size is retrieved using the normalized difference grain size index (NDGSI; bands two and five), from which the clean snow albedo is modeled. The MODIS spectrum is then matched to the modeled clean snow spectrum at band 2 (841–876 nm). Snow darkening is calculated by integrating the difference between the observed and clean snow spectrum. Finally, RF_{dust} (Wm^{-2}; Figure 1) is calculated by multiplying snow darkening by the modeled clear-sky solar irradiance, at the time of MODIS overpass, over the same wavelength range.

The MODDRFS retrievals are based on whole pixel reflectance, which are artificially inflated by darker snow free surfaces, such as bare ground and vegetation, in mixed pixels (Painter, Bryant, & Skiles, 2012). To ensure a robust analysis, only pixels with high snow cover should be analyzed, otherwise mixed pixel effects would dominate. Here, pixels with ≥95% snow cover and continuous persistence of over 5 days were analyzed. These thresholds limit error and bias introduced by darker land cover types on RF_{dust} retrievals.

2.2. Methods

2.2.1. Time Series and Spatial Analysis

For every day over the MODIS record (2001–2023), in each pixel that met threshold levels, RF_{dust} was calculated within the UCRB boundary. The central tendency of the data was summarized at daily and monthly scales using the basin wide median values. The annual trends were analyzed; however, our analysis largely focuses on RF_{dust} in April and May, which we refer in combination as spring. Spring is when dust impacts are most relevant for melt, when snow cover is widespread across much of the mountain headwaters, and when dust emission is most intense from the Colorado Plateau (Hennen et al., 2022). Snow depletion typically occurs after May; however, fewer pixels remain that meet threshold requirements late in the melt season. At the annual scale, a seasonal Mann Kendall (M-K) test and Sen slope were used to assess and quantify trends in the continuous daily basin wide median RF_{dust} values, which were not normally distributed. In spring, when values were closer to normally

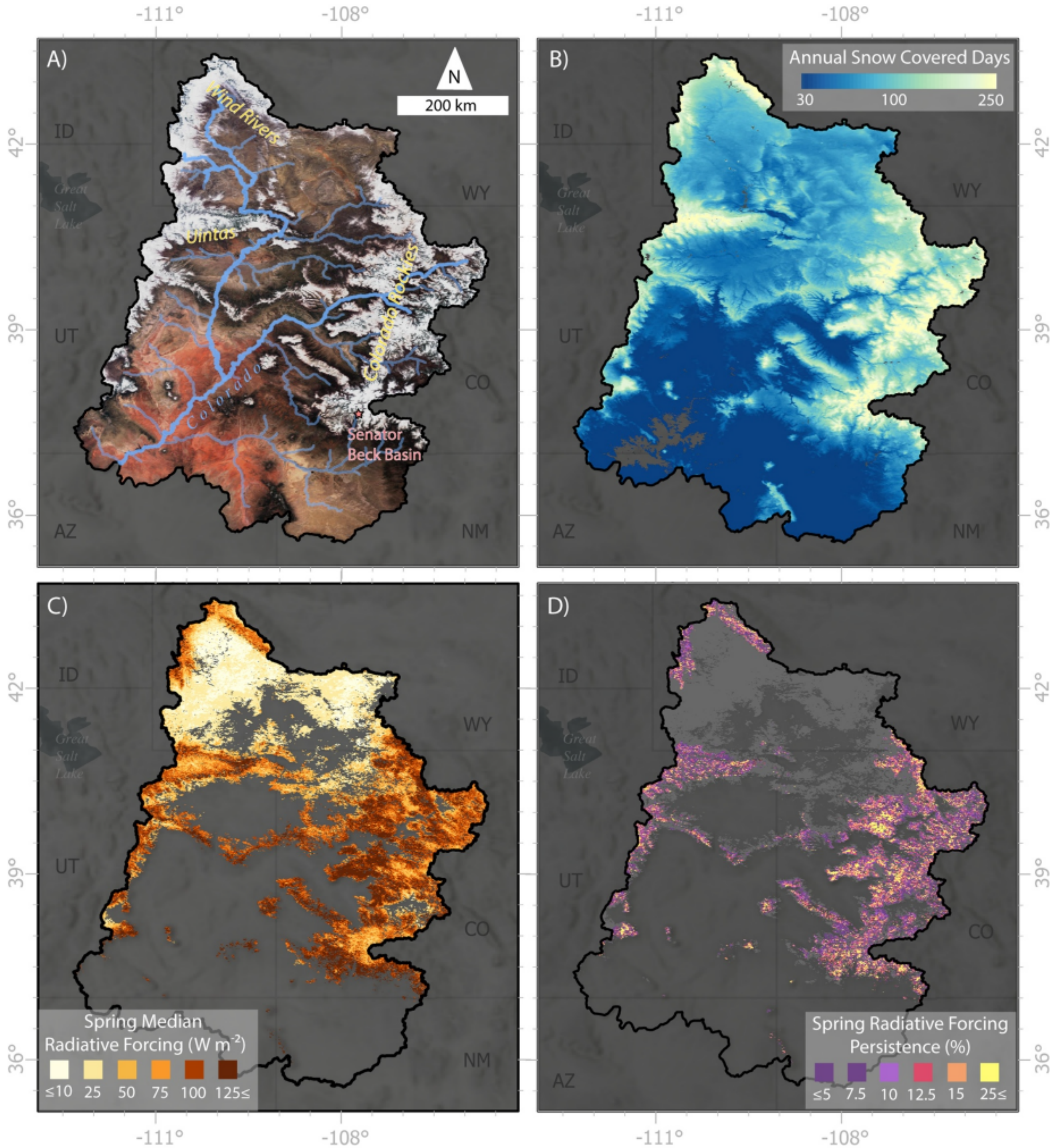

Figure 1. Overview maps of the Upper Colorado Basin (UCRB), outlined in black. (a) The major UCRB waterways overlaid on satellite imagery from April 2022 visualizing typical extent of springtime snow cover. Over the MODIS record, (b) annual snow covered days visualizing extent and duration of snow cover, (c) spring RF_{dust}, and (d) persistence of RF_{dust} (% of time above 50 Wm^{-2}).

distributed, a traditional M-K trend test and Sen's slope were used to assess trends on the continuous basin median RF_{dust} timeseries.

The RF_{dust} can be converted into a melt contribution when divided by the latent heat of fusion of water (334 kJ kg^{-1}), the energy required to change water from solid to liquid, assuming the snow is already at melting point (0°C). This has been used in previous studies to assess the direct contribution of snow darkening to melt rates at local scales (Kaspari et al., 2015; Painter et al., 2013) but has not yet been applied to remote sensing retrievals. The melt contribution, calculated in each pixel for the hour of MODIS overpass, is in units of kg m^{-2}, equivalent to millimeter of snow water equivalent per hour (mm w.e. hr^{-1}). Additionally, for broader context

10.1029/2024GL112757

across different RF_{dust} scenarios, the hourly metrics were extended to daily metrics by accounting for hourly changes in solar radiation. Calculations used an average idealized clear sky spring day, 12 hr in length, with peak solar noon irradiance of 1,000 Wm^{-2}.

To visualize spatial patterns, record median spring RF_{dust} and persistence, the percent of time pixel RF_{dust} was above 50 Wm^{-2}, were mapped over the UCRB (Figure 1). To assess how dust impacts vary with elevation and latitude across the UCRB, a 90 m DEM of the WUS (Hanser, 2008) was reprojected and resampled to match the MODIS grid. Mean elevation and latitude were associated with each MODIS pixel, and patterns were assessed by binning RF_{dust} by 20 m elevation bands and 0.05° latitude bands. The full record median values were then compared to high and low dust RF_{dust} years to assess differences in spatial patterns. We also use the date of maximum RF_{dust} ($date_{MaxRF}$) as a useful metric for evaluating the timing of RF_{dust} intensification. For context, typically the $date_{MaxRF}$ occurs when dust layers have combined at the surface, which occurs during snowmelt progression, and will relate to where dust layers are relative to surface, how quickly melt progresses to expose dust layers, and how frequently spring snowfall buries dust.

3. Results

In the spring median RF_{dust} varies spatially from <10 Wm^{-2} to >125 Wm^{-2}, with persistent RF_{dust} areas confined to mountainous areas (Figure 1). The RF_{dust} persistence pattern relates to deeper mountain snowpacks, due to longer snow duration the snow can "collect" more dust events and subsequently that dust will be exposed for longer. Generally, the lowest and least persistent RF_{dust} values occur in the northern Uinta (UT) and Wind River Range (WY). The highest and most persistent values occur in the central to southern Colorado Rockies, where RF_{dust} can have the largest impact on melt rates, as it is the largest extent of snow cover in the UCRB. The temporal and spatial variability in RF_{dust} and $melt_{dust}$ magnitudes over the record is presented in more detail in individual sections below. For uncertainty characterization an assessment of remotely sensed RF_{dust} against 19 years of in situ RF_{dust} observations (2005–2023) at SBBSA is presented in SI; in summary, the MAE was 17 Wm^{-2} and RMSE was 50 Wm^{-2}.

3.1. Temporal Patterns

The general temporal patterns in basin wide RF_{dust} were similar every year and mirror previous observations; RF_{dust} remained low through the accumulation season and then intensified as melt progressed and dust accumulated at the surface over the spring season (Figure 2a). The highest RF_{dust} values occurred at the end of spring; in individual pixels RF_{dust} values can reach above 400 Wm^{-2}, and in many years high end of season values introduced a positive skew into the distribution of spring values (Table S1 in Supporting Information S1). The basin wide, full record, spring median RF_{dust} was 77 Wm^{-2} with values as high as 91 Wm^{-2} in 2009 (+14 Wm^{-2} from median) and as low as 62 Wm^{-2} in 2017 (−15 Wm^{-2} from median). In May, the RF_{dust} values were always higher (April = 67 Wm^{-2}, May = 96 Wm^{-2}) and consistently had a wider spread of values (range/st. dev April = 29/7 Wm^{-2}, May = 48/13 Wm^{-2}).

3.1.1. Seasonal Variability

The timing and magnitude of RF_{dust} intensification varied from year to year with weather, snow depth, melt initiation, dust deposition timing, and dust layer exposure (Figure 2a). Relatedly, the relationship between April and May RF_{dust} indicated that April RF_{dust} was not a strong predictor for May values (median $R^2 = 0.2$). For example, in 2006, April RF_{dust} was near median but then increased in May to well above median (Table S1 in Supporting Information S1). This corresponds to previously observed timing of dust layer exposure and intensifying RF_{dust} values in 2006 across the month of May (Painter, Skiles, et al., 2012; Skiles et al., 2012). In contrast, in 2012, both April and May RF_{dust} were well above the median. This also corresponds with the observation record; dust events were only observed in March and April, and with minimal new snowfall to reset values in May, the darkening impact was sustained (Skiles et al., 2015). In years when dust impacts were relatively low, including 2015–2017, April RF_{dust} was near or slightly below median, with minimal RF_{dust} intensification in May. This was particularly pronounced in 2015, a low snow year that had early melt out in the southern portion of the basin. In contrast, 2023 was a near record snow year, and RF_{dust} was low in April due to frequent snowfall, but as snow started to melt in May, RF_{dust} doubled and was above median.

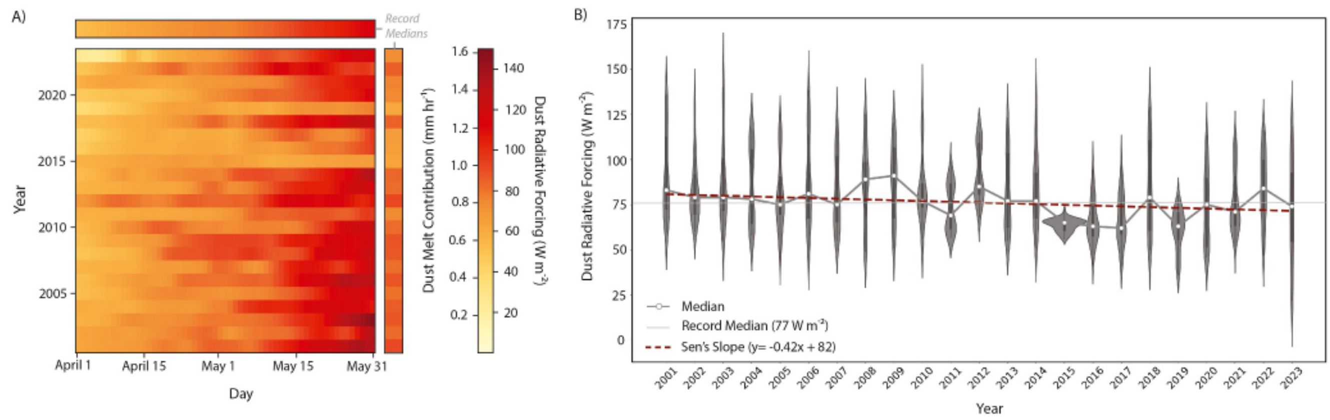

Figure 2. Spring UCRB RF_{dust} patterns over the MODIS record. (a) Daily surface plot of median RF_{dust} and corresponding melt contribution. The secondary summary bars visualize the daily (above) and annual (right) median values. (b) Distributions of median RF_{dust} as violin plots each spring, with record median and trend line.

3.1.2. Record-Length Patterns

The basin wide median spring RF_{dust} and distribution of values show interannual variability over the MODIS record. A comparison to snow extent patterns did not indicate a direct relationship with snow cover. However, the year-to-year patterns in spring RF_{dust} suggest that there could be broader (i.e., climate scale) controls on RF_{dust} with clustering of years with similar distributions and magnitude of median values (Figure 2b). Generally, during the first half of the record there were more years with above median spring RF_{dust}, and subsequently, the more recent part of the record spring RF_{dust} had more years below the median (Figure 2b). Due to this pattern, median RF_{dust} has a decreasing trend over the full annual and spring median RF_{dust} records (annual $y = -0.28x+40$, spring Sen's $y = -0.42x+82$). Although both trends were significant (M-K $P < 0.05$) the magnitudes of decreases indicated by Sen's slope from year to year were slight (<1 Wm^{-2}) relative to RF_{dust} magnitudes and uncertainty.

3.1.3. Melt Contribution

Snowmelt was accelerated by RF_{dust} every spring over the MODIS record. The corresponding $melt_{dust}$ for the basin wide record median RF_{dust} was 0.8 mm w.e. hr^{-1} at time of MODIS overpass, equating to daily melt of 6 mm w.e. when accounting for variation in clear sky solar radiation over the course of a day. This impact varies from year-to-year, with interannual variability in RF_{dust}. In the relatively low impact dust year of 2019, the basin-wide spring median $melt_{dust}$ was 0.7 mm w.e. hr^{-1} and maximum $melt_{dust}$ was 0.9 mm w.e. hr^{-1} over the basin, corresponding to a daily median $melt_{dust}$ of 5.2 mm and maximum of 6.5 mm per day. In contrast, in 2009, a high impact dust year, the basin-wide median and maximum $melt_{dust}$ were 1.0 mm w.e. hr^{-1} and 1.3 mm w.e. hr^{-1} translating into a daily $melt_{dust}$ contribution of 7.4 and 10 mm per day. The $melt_{dust}$ efficacy was notably ∼30% greater in 2009 relative to 2019. For broader context, the melt due to total net solar radiation on a typical spring day, assuming an albedo of 0.8, would be ∼2 mm w.e. hr^{-1} (∼15 mm per day). Observed melt rates could be slower or faster depending on other energy balance contributions.

3.2. Spatial Patterns

The record median values show that RF_{dust} was most intense in elevations between 2,800 and 3,600 m and south of 41°N (Figure 3a). This means that the largest dust impacts in the UCRB occurred in the Colorado Rockies with lower impacts in the Uinta Mountains and Wind River Range (Figures 1 and 3a). North of 41°N, median RF_{dust} values were typically around 50 Wm^{-2}, whereas south 41°N values were more typically around 80 Wm^{-2}, with values in some pixels approaching 200 Wm^{-2} (1.16 mm w.e. hr^{-1}). Dust was still relevant for melt in the northern ranges, albeit to a lesser degree; the lowest median RF_{dust} equates to ∼0.5 mm w.e. hr^{-1} (4 mm of melt per day). There was also a decreasing gradient with elevation, the lowest median RF_{dust} values occurred at the highest elevations, between 3,800 and 4,200 m, with median values of ∼25 Wm^{-2} (0.27 mm hr^{-1}) (Figure 3a).

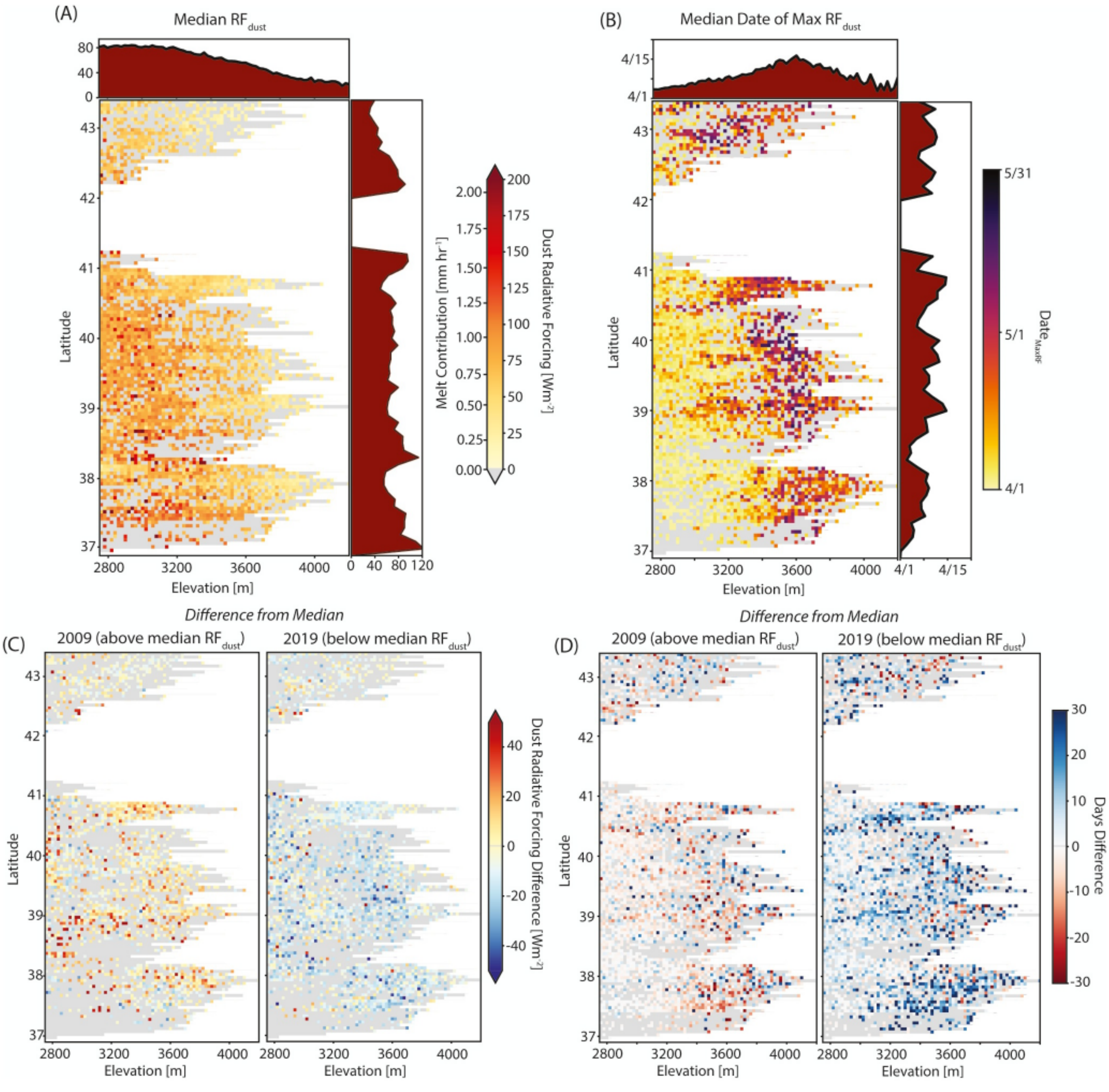

Figure 3. Spatial distribution of dust on snow impact metrics as a function of latitude (*y*-axis) and elevation (*x*-axis). Gray represents terrain where no RF_{dust} values were retrieved. (a) Record spring median RF_{dust} and $melt_{dust}$ and (b) record median $date_{MaxRF}$. Supplementary plots show distribution of values per latitude and elevation bin. (c) Difference from record median RF_{dust} and (d) difference from record median $date_{MaxRF}$ for 2009 (high dust) and 2019 (low dust).

Relative to record median, the high dust year of 2009 generally had consistently above median RF_{dust} across most of the basin (Figure 3c). However, there were interesting RF_{dust} difference patterns, for example, the most elevated values occurred south of 39°N, indicating the most intense impacts still occur in the southern part of the basin. It is notable that at higher elevations, where dust impacts generally tend to be lower, 2009 RF_{dust} was consistently above median by ~20 Wm^{-2}. In a low dust year, 2019, RF_{dust} was generally at or below median across the entire basin with more muted differences relative to record medians (Figure 3c). The RF_{dust} was relatively consistent during spring of 2019, suggesting less variability in dust deposition and exposure (Figure 2a). There were areas, in the 3,400–3,800 m elevation band and between 39°N and 40°N, where RF_{dust} values were 20–40 Wm^{-2} lower than median.

The date on which RF_{dust} peaks can range from early April to late May. Generally, in lower elevations (below 3,200 m) $date_{MaxRF}$ occurred earlier relative to higher elevations, where snowmelt would initiate later. The elevation band at which $date_{MaxRF}$ occurred latest is ~3,600 m, with a small number of pixels at the highest elevations showing earlier $date_{MaxRF}$ likely due to shallow, wind impacted, alpine snow cover. In terms of latitude, earliest $date_{MaxRF}$ occurred south of 38°N, with median $date_{MaxRF}$ around May 1st, with peak happening a week or two later for the mountains north of 38°N (Figure 3b).

There were interesting patterns in the $date_{MaxRF}$ between high and low dust years (Figure 3d). Both exhibited a latitudinal gradient. In 2009, $date_{MaxRF}$ occurred 1–2 weeks earlier than median south of 41°N. This was most pronounced in the southern Colorado Rockies, where $date_{MaxRF}$ happened ~3 weeks earlier, likely related to high RF_{dust} accelerating snowmelt. The more northern extent of the basin was generally near or later then median $date_{MaxRF}$. In 2019, the $date_{MaxRF}$ occurred later, by 1–2 weeks, than the median across most of the basin, with the exception the mountains north of 41° where it was also near or later then median (Figure 3f).

4. Uncertainty and Considerations

The factors contributing to MODDRFS uncertainty retrievals are discussed in detail in Painter, Bryant, and Skiles (2012). Briefly, uncertainties primarily relate to, (a) spectral resolution, the step-like spectra do not fully resolve snow reflectance features and how they vary with snow properties, and (b) spatial resolution, in mountains snow is highly heterogenous and commonly mixed with other land surface types. Other uncertainties include atmospheric correction, geolocation error, sensor zenith angle, and snow surface characteristics (Painter, Bryant, & Skiles, 2012).

In addition to the advantage of a longer period of analysis, this study also used the continuous daily gap-filled STC products. The comparison to in situ RF_{dust} values shows similar performance to Painter, Bryant, & Skiles, 2012, with a positive bias at low RF_{dust} and negative bias at high RF_{dust}. There are some likely explanations for these patterns. Of note is the fact that products rely on the assumption of clear sky incoming solar irradiance, not accounting for lower irradiance under cloudy conditions, which would produce a positive bias. Additionally, RF_{dust} can only be analyzed up to MODIS band 2 (841–876 nm) and at high dust concentrations the darkening impact extends past this wavelength range (Skiles et al., 2018), which would produce a negative bias.

Due to the inherent limitations of the remote sensing data set, Painter, Bryant, and Skiles (2012) described MODDRFS retrievals as semi-quantitative. Relatedly, Warren (2013) posits that multispectral satellites are not suitable for detecting albedo declines due to LAPs except for the most heavily impacted regions. The UCRB is one such region and for this study the strengths of MODIS, including near daily temporal resolution and 23-year record length, outweigh the weaknesses. Ultimately, given the high uncertainties, we are more confident in overall patterns, as opposed to absolute values. For future studies, the limitations presented here should be considered. Specifically, the RMSE is ~50 Wm^{-2} and RF_{dust} retrievals do not reach 0 Wm^{-2} but rather have a baseline value around 25 Wm^{-2} (see Figure 3b and Supporting Iinformation S1). This can be related to multiple factors but is primarily due to coarse spatial resolution (~500 m) that rarely captures fully clean snow-covered pixels in mountain environments. Given these values, we suggest retrievals should only be used to interpret RF_{dust} trends in regions, and over time periods, where RF_{dust} values reach and sustain relatively high values (>50 Wm^{-2}). This would limit application primarily to mid-latitude mountain snow cover near and upwind from LAP sources (Skiles et al., 2018).

It is important to note that although dust is in the name of the MODDRFS algorithm, the model cannot differentiate between LAPs contributing to surface darkening. Based on detailed study of LAP concentrations and RF_{dust} contributions (Skiles & Painter, 2017, 2018), analysis of absorption by particles deposited in snow (Reynolds et al., 2020), and detailed modeling of LAP transport to snow (Qian et al., 2009), we know that dust is the dominant LAP during the spring melt season in this region. That may not be the case in other LAP impacted regions, for example, the south slope of the Himalaya, which is downwind from large populations centers and arid regions, with relatively large input of black carbon, brown carbon, and dust (Gertler et al., 2016; Ramachandran et al., 2020; Sarangi et al., 2020).

Finally, a risk to continued spatiotemporal RF_{dust} analysis is that MODIS is operating past the expected life span. We plan to develop RF_{dust} retrievals for other multispectral satellites, extending the length of this record the NOAA Visible Infrared Imaging Suite (VIIRS), as well as exploring patterns at finer spatial scales using Landsat-

OLI instruments (8 and 9). Additionally, in the upcoming decade it is expected that both NASA and ESA will launch imaging spectrometers that will provide global coverage of fully resolved spectral reflectance of the Earth's surface, which are expected to reduce uncertainty in snow retrievals, including RF_{dust}, based on results at the airborne scale (Donahue et al., 2023; Painter et al., 2013).

5. Discussion and Conclusion

The UCRB RF_{dust} patterns exhibited spatial and temporal variability over the 23-year MODIS record; across elevation bands there was a ~40 Wm^{-2} range in median spring RF_{dust}, greater differences (~80 Wm^{-2}) across latitudinal bands, and a ~30 Wm^{-2} range between highest and lowest impact years. Relevant patterns emerged from the analysis that will be helpful in generalizing dust impacts and putting them in context relative to the observation record. For example, RF_{dust} tends to peak earliest and be most intense in the southern portion of the basin, which is proximal to dust producing regions, where there is more mountainous terrain. In terms of elevation, dust impacts tend to be largest in the lower alpine elevations, 2,800–3,500 m, where there is the most snow-covered area. The long-term observation record at SBBSA is located where impacts are most intense and therefore should not be considered representative of the broader headwaters, particularly the northern UCRB.

Across the full record dust was a relevant, but variable, contributor to snowmelt with median spring RF_{dust} accelerating melt by nearly 1 mm w.e. hr^{-1}. There is no predictive capability to forecast the magnitude of dust impacts in any given spring, and therefore, it would be valuable to leverage remote sensing retrievals to inform hydrologic prediction. Unfortunately, there is no direct way to account for snow darkening in SNOW-17, the temperature-index snow model used in operational forecasting by the Colorado Basin River Forecast Center (Bryant et al., 2013), although increased temperature can be used as a proxy for dust impacts. However, process-based models are under development that can be directly informed by remote sensing retrievals (e.g., Meyer et al., 2024). More accurate forecasting and allocation of snow water resources has important policy implications; the Colorado River system is under extreme pressure from changing climate and populations with California, Nevada, and Arizona agreeing to cut their water received by ~13% by 2026 (Department of the Interior).

One interesting aspect of this analysis was the pattern of higher RF_{dust} in the first part of the MODIS record, with relatively lower RF_{dust} more recently, producing a slight but statistically significant decreasing trend over the record. These patterns do not align with periods of drought in the Colorado River Basin, as identified by the US Drought Monitor (https://droughtmonitor.unl.edu/), indicating that there is not a straightforward relationship between aridity and dust. However, the MODIS record corresponds to the ongoing two-decade long megadrought in the WUS that started in 2000 (Szejner et al., 2020, 2021; Williams et al., 2020), making it challenging to know what is "normal" at longer time scales. Studies evaluating dust emissions from the Colorado Plateau found a similar decreasing trend in dust emissions following 2014 (Hand et al., 2017; Hennen et al., 2023). Although the direct causes remain unclear, the hypothesis is that it relates to a combination of increasing surface roughness (vegetation) and decreasing wind speeds related to climate variability (Hennen et al., 2023). Links to land use change, climate scale variability, and other factors that influence dust emission and transport merit further study to better understand the full life cycle of dust on snow and impacts on snow water resources and hydrology in the Colorado River Basin.

Data Availability Statement

The Senator Beck Basin Study Area data is available from the Center for Snow and Avalanche Studies (https://snowstudies.org/archival-data/). Processed datasets, available via Zenodo, include post-processed hourly corrected radiation and radiative forcing (Skiles, 2024) and direct radiative forcing at time of MODIS overpass (Naple, 2023). There is an open-access Jupyter notebook containing the processing workflow used for this analysis (https://github.com/UofU-Cryosphere/MODDRFS_processing).

Acknowledgments

This study was funded by NASA Interdisciplinary Science in Earth Science Grant 80NSSC20K1672 and NSF Division of Earth Sciences Award 2012091. The Institute for Arctic and Alpine Research, the Snow Today team and Operations and User Services at the National Snow and Ice Data Center, the Research Computing of the University of Colorado Boulder made data available with NASA Grants 80NSSC18K0427, 80NSSC22K0703, 80NSSC22K0929. We would like to thank the Center for Snow and Avalanche Studies for maintenance of Senator Beck Basin Study Area and providing in situ data sets used in this study. The resources from the Center for High Performance Computing at the University of Utah are gratefully acknowledged.

References

Barnett, T. P., & Pierce, D. W. (2009). Sustainable water deliveries from the Colorado River in a changing climate. *Proceedings of the National Academy of Sciences*, *106*(18), 7334–7338. https://doi.org/10.1073/pnas.0812762106

Brahney, J., Ballantyne, A. P., Sievers, C., & Neff, J. C. (2013). Increasing Ca2+ deposition in the western US: The role of mineral aerosols. *Aeolian Research*, *10*, 77–87. https://doi.org/10.1016/j.aeolia.2013.04.003

Bryant, A. C., Painter, T. H., Deems, J. S., & Bender, S. M. (2013). Impact of dust radiative forcing in snow on accuracy of operational runoff prediction in the Upper Colorado River Basin. *Geophysical Research Letters*, *40*(15), 3945–3949. https://doi.org/10.1002/grl.50773

Donahue, C. P., Menounos, B., Viner, N., Skiles, S. M. K., Beffort, S., Denouden, T., et al. (2023). Bridging the gap between airborne and spaceborne imaging spectroscopy for mountain glacier surface property retrievals. *Remote Sensing of Environment*, *299*, 113849. https://doi.org/10.1016/J.RSE.2023.113849

Dozier, J., Painter, T. H., Rittger, K., & Frew, J. E. (2008). Time-space continuity of daily maps of fractional snow cover and albedo from MODIS. *Advances in Water Resources*, *31*(11), 1515–1526. https://doi.org/10.1016/j.advwatres.2008.08.011

Gertler, C. G., Puppala, S. P., Panday, A., Stumm, D., & Shea, J. (2016). Black carbon and the Himalayan cryosphere: A review. *Atmospheric Environment*, *125*, 404–417. https://doi.org/10.1016/J.ATMOSENV.2015.08.078

Hand, J. L., Gill, T. E., & Schichtel, B. A. (2017). Spatial and seasonal variability in fine mineral dust and coarse aerosol mass at remote sites across the United States. *Journal of Geophysical Research*, *122*(5), 3080–3097. https://doi.org/10.1002/2016JD026290

Hanser, S. E. (2008). *Elevation in the western United States (90 meter DEM)*. Wiley.

Hennen, M., Chappell, A., Edwards, B. L., Faist, A. M., Kandakji, T., Baddock, M. C., et al. (2022). A North American dust emission climatology (2001–2020) calibrated to dust point sources from satellite observations. *Aeolian Research*, *54*, 100766. https://doi.org/10.1016/j.aeolia.2021.100766

Hennen, M., Chappell, A., & Webb, N. P. (2023). Modelled direct causes of dust emission change (2001–2020) in southwestern USA and implications for management. *Aeolian Research*, *60*, 100852. https://doi.org/10.1016/j.aeolia.2022.100852

Hock, R., Rasul, G., Adler, C., Cáceres, B., Gruber, S., Hirabayashi, Y., et al. (2019). *High mountain areas chapter—IPCC Special report on the oceans and cryosphere in a changing climate (SROCC)*. Intergovernmental Panel on Climate Change (IPCC).

Jacobs, J., Dzombak, D. A., Platt, R. H., Habibian, M., & Galloway, G. E. (2011). The sustainability of water resources in the Colorado River Basin nutrient control in large-scale U.S. Watersheds: The Chesapeake Bay and northern Gulf of Mexico managing sustainable water supplies: The New York City and Metropolitan Boston experience critical issues and sustainability challenges for a large metropolitan water-wastewater facility a plea for a coordinated national water policy. Retrieved from http://www.nae.edu/TheBridge

James, T., Evans, A., Madly, E., & Kelly, C. (2014). *The economic importance of the Colorado river to the basin region. Final Rep., L. William Seidman Research Institute* (Vol. 54). Arizona State University.

Jensen, A. S., Rittger, K., & Raleigh, M. S. (2024). Spatio-temporal patterns and trends in MODIS-retrieved radiative forcing by snow impurities over the Western US from 2001 to 2022. *Environmental Research: Climate*, *3*(2), 025001. https://doi.org/10.1088/2752-5295/ad285a

Kaspari, S., Skiles, S. M. K., Delaney, I., Dixon, D., & Painter, T. H. (2015). Accelerated glacier melt on Snow Dome, Mount Olympus, Washington, USA, due to deposition of black carbon and mineral dust from wildfire. *Journal of Geophysical Research*, *120*(7), 2793–2807. https://doi.org/10.1002/2014JD022676

Landry, C. C., Buck, K. A., Raleigh, M. S., & Clark, M. P. (2014). Mountain system monitoring at Senator Beck Basin, San Juan Mountains, Colorado: A new integrative data source to develop and evaluate models of snow and hydrologic processes. *Water Resources Research*, *50*(2), 1773–1788. https://doi.org/10.1002/2013WR013711

Meyer, J., Hedrick, A., & Skiles, S. M. (2024). A new approach to net solar radiation in a spatially distributed snow energy balance model to improve snowmelt timing. *Journal of Hydrology*, *638*, 131490. https://doi.org/10.1016/j.jhydrol.2024.131490

Naple, P. (2023). Senator Beck Basin radiative forcing at MODIS overpass (2005-2022 WY) [Dataset]. *Zenodo*. https://doi.org/10.5281/zenodo.10038176

Neff, J. C., Ballantyne, A. P., Farmer, G. L., Mahowald, N. M., Conroy, J. L., Landry, C. C., et al. (2008). Increasing eolian dust deposition in the western United States linked to human activity. *Nature Geoscience*, *1*(3), 189–195. https://doi.org/10.1038/ngeo133

Painter, T. H., Barrett, A. P., Landry, C. C., Neff, J. C., Cassidy, M. P., Lawrence, C. R., et al. (2007). Impact of disturbed desert soils on duration of mountain snow cover. *Geophysical Research Letters*, *34*(12). https://doi.org/10.1029/2007GL030284

Painter, T. H., Bryant, A. C., & Skiles, S. M. (2012). Radiative forcing by light absorbing impurities in snow from MODIS surface reflectance data. *Geophysical Research Letters*, *39*(17). https://doi.org/10.1029/2012GL052457

Painter, T. H., Deems, J. S., Belnap, J., Hamlet, A. F., Landry, C. C., & Udall, B. (2010). Response of Colorado River runoff to dust radiative forcing in snow. *Proceedings of the National Academy of Sciences*, *107*(40), 17125–17130. https://doi.org/10.1073/pnas.0913139107/-/DCSupplemental

Painter, T. H., Rittger, K., McKenzie, C., Slaughter, P., Davis, R. E., & Dozier, J. (2009). Retrieval of subpixel snow covered area, grain size, and albedo from MODIS. *Remote Sensing of Environment*, *113*(4), 868–879. https://doi.org/10.1016/j.rse.2009.01.001

Painter, T. H., Seidel, F. C., Bryant, A. C., McKenzie Skiles, S., & Rittger, K. (2013). Imaging spectroscopy of albedo and radiative forcing by light-absorbing impurities in mountain snow. *Journal of Geophysical Research: Atmospheres*, *118*(17), 9511–9523. https://doi.org/10.1002/jgrd.50520

Painter, T. H., Skiles, S. M. K., Deems, J. S., Brandt, W. T., & Dozier, J. (2018). Variation in rising limb of Colorado river snowmelt runoff hydrograph controlled by dust radiative forcing in snow. *Geophysical Research Letters*, *45*(2), 797–808. https://doi.org/10.1002/2017GL075826

Painter, T. H., Skiles, S. M. K., Deems, J. S., Bryant, A. C., & Landry, C. C. (2012). Dust radiative forcing in snow of the upper Colorado River Basin: 1. A 6 year record of energy balance, radiation, and dust concentrations. *Water Resources Research*, *48*(7). https://doi.org/10.1029/2012WR011985

Qian, Y., Gustafson, W. I., Leung, L. R., & Ghan, S. J. (2009). Effects of soot-induced snow albedo change on snowpack and hydrological cycle in western United States based on weather research and forecasting chemistry and regional climate simulations. *Journal of Geophysical Research*, *114*(3). https://doi.org/10.1029/2008JD011039

Ramachandran, S., Rupakheti, M., & Lawrence, M. G. (2020). Black carbon dominates the aerosol absorption over the Indo-Gangetic Plain and the Himalayan foothills. *Environment International*, *142*, 105814. https://doi.org/10.1016/J.ENVINT.2020.105814

Rasmussen, R., Baker, B., Kochendorfer, J., Meyers, T., Landolt, S., Fischer, A. P., et al. (2012). How well are we measuring snow: The NOAA/FAA/NCAR winter precipitation test bed. *Bulletin of the American Meteorological Society*, *93*(6), 811–829. https://doi.org/10.1175/BAMS-D-11-00052.1

Reynolds, R. L., Goldstein, H. L., Moskowitz, B. M., Kokaly, R. F., Munson, S. M., Solheid, P., et al. (2020). Dust deposited on snow cover in the San Juan mountains, Colorado, 2011–2016: Compositional variability bearing on snow-melt effects. *Journal of Geophysical Research: Atmospheres*, *125*(7). https://doi.org/10.1029/2019JD032210

Rittger, K., Lenard, S. J., Palomaki, R. T., Brodzik, M. J., Stillinger, T., Bair, E. H., et al. (2024). *Historical MODIS/Terra L3 Global Daily 500m SIN Grid Snow Cover, Snow Albedo, and Snow Physical Properties. (STC_MODSCGDRF_HIST, Version 1)*. National Snow and Ice Data Center. https://doi.org/10.7265/f6j3-f387

Sarangi, C., Qian, Y., Rittger, K., Ruby Leung, L., Chand, D., Bormann, K. J., & Painter, T. H. (2020). Dust dominates high-altitude snow darkening and melt over high-mountain Asia. *Nature Climate Change*, *10*(11), 1045–1051. https://doi.org/10.1038/s41558-020-00909-3

Skiles, S. M. (2024). Senator Beck Basin corrected radiation (water years 2005-2023) (version 2) [Dataset]. *Zenodo*. https://doi.org/10.5281/zenodo.14675762

Skiles, S. M., Flanner, M., Cook, J. M., Dumont, M., & Painter, T. H. (2018). Radiative forcing by light-absorbing particles in snow. In *Nature climate change* (Vol. 8(11), pp. 964–971). Nature Publishing Group. https://doi.org/10.1038/s41558-018-0296-5

Skiles, S. M., & Painter, T. (2017). Daily evolution in dust and black carbon content, snow grain size, and snow albedo during snowmelt, Rocky Mountains, Colorado. *Journal of Glaciology*, *63*(237), 118–132. https://doi.org/10.1017/jog.2016.125

Skiles, S. M., & Painter, T. (2018). Assessment of radiative forcing by light-absorbing particles in snow from in situ observations with radiative transfer modeling. *Journal of Hydrometeorology*, *19*(8), 1397–1409. https://doi.org/10.1175/JHM-D-18-0072.1

Skiles, S. M., Painter, T. H., Belnap, J., Holland, L., Reynolds, R. L., Goldstein, H. L., & Lin, J. (2015). Regional variability in dust-on-snow processes and impacts in the Upper Colorado River Basin. *Hydrological Processes*, *29*(26), 5397–5413. https://doi.org/10.1002/hyp.10569

Skiles, S. M., Painter, T. H., Deems, J. S., Bryant, A. C., & Landry, C. C. (2012). Dust radiative forcing in snow of the upper Colorado River Basin: 2. Interannual variability in radiative forcing and snowmelt rates. *Water Resources Research*, *48*(7). https://doi.org/10.1029/2012WR011986

Szejner, P., Belmecheri, S., Babst, F., Wright, W. E., Frank, D. C., Hu, J., & Monson, R. K. (2021). Stable isotopes of tree rings reveal seasonal-to-decadal patterns during the emergence of a megadrought in the Southwestern US. *Oecologia*, *197*(4), 1079–1094. https://doi.org/10.1007/s00442-021-04916-9

Szejner, P., Belmecheri, S., Ehleringer, J. R., & Monson, R. K. (2020). Recent increases in drought frequency cause observed multi-year drought legacies in the tree rings of semi-arid forests. *Oecologia*, *192*(1), 241–259. https://doi.org/10.1007/s00442-019-04550-6

Warren, S. G. (2013). Can black carbon in snow be detected by remote sensing? *Journal of Geophysical Research: Atmospheres*, *118*(2), 779–786. https://doi.org/10.1029/2012JD018476

Williams, A. P., Cook, E. R., Smerdon, J. E., Cook, B. I., Abatzoglou, J. T., Bolles, K., et al. (2020). Large contribution from anthropogenic warming to an emerging North American megadrought. *Science*, *368*(6488), 314–318. https://doi.org/10.1126/science.aaz9600